Vol. 67: 209–220, 2016
doi: 10.3354/cr01376

CLIMATE RESEARCH
Clim Res

Published March 14

A tree-ring chronology spanning 210 years in the coastal area of southeastern China, and its relationship with climate change

Yingjun Li[1,2], Keyan Fang[1,3,*], Chunfu Cao[1], Dawen Li[1], Feifei Zhou[1], Zhipeng Dong[1], Yu Zhang[1], Zhanfeng Gan[1]

[1]Institute of Geography, Key Laboratory of Humid Subtropical Eco-geographical Process (Ministry of Education), College of Geographical Sciences, Fujian Normal University, Fuzhou 350007, China

[2]Research Center for Scientific Development in the Fenhe River Valley, Taiyuan Normal University, Jinzhong 030619, China

[3]Key Laboratory of Cenozoic Geology and Environment, Institute of Geology and Geophysics, Chinese Academy of Sciences, Beijing 100029, China

ABSTRACT: A 210 yr tree-ring chronology (1804–2013) was developed from *Pinus massoniana* trees at Gu Mountain of Fujian Province in southeastern China, which is the nearest chronology to the coastal area of the East China Sea. The highest correlations with monthly climate variables were observed for precipitation in the current (i.e. the same year as the tree-ring growth) July and September, and the highest correlation with seasonal climate variables was found with precipitation from the current period June to September. We found a shift between the climate–growth correlations before and after 1977. From 1953–1977, tree growth was mainly limited by precipitation in the current June and September. In addition, the highest correlation with seasonal precipitation was from the current June to September. However, from 1978–2013, tree growth was negatively correlated with temperature in the current June and July and positively correlated with January temperature and July precipitation, with the highest negative correlation occurring with seasonal temperature from June to August of the current year. A sharp increase in temperature and decline in light precipitation with more frequent heavy rain and storm-associated rain enhanced the summer drought from 1978–2013. In addition, more cold snaps in January played a role in limiting tree growth from 1978–2013. This chronology shows significant positive correlations with those of the El Niño-Southern Oscillation (ENSO), Pacific Decadal Oscillation (PDO), and East Asia Summer Monsoon (EASM) indexes, especially in their decadal variations. At an annual time scale, a warm ENSO may cause a weak EASM in the positive PDO phase, and a weak EASM may decrease precipitation, raise temperature, and further limit tree growth. At a decadal time scale, the weakening EASM has promoted tree growth by the center-southward-moving monsoon rain since 1977.

KEY WORDS: Tree-ring · Precipitation · Southeastern China · ENSO

1. INTRODUCTION

The climate in southeastern China exhibits great variability in response to the dynamics of the Asian summer monsoon, which has a strong impact on the most populated region in China (Ding et al. 2010, Chen et al. 2013a). However, the limited instrumental data that exists (i.e. that of a few decades) has restricted our efforts to disentangle the influences of human activities with those of nature, highlighting the need to infer long-term climate variations from proxies. Tree rings have been widely used to reconstruct paleoclimatic changes due to their high sensitivity to climate, accurate dating capacity and exten-

*Corresponding author: kfang@fjnu.edu.cn

sive spatial coverage (Hughes et al. 2011). Although numerous tree-ring chronologies have been published in China, most have been created from locations in the arid, cold west and north of China (Gou et al. 2007, Liang et al. 2010, Y. Liu et al. 2010, Shao et al. 2010, Chen et al. 2013b, H. Liu et al. 2013, Yang et al. 2014, X. Liu et al. 2014, Zhang et al. 2015). Few tree-ring chronologies have been generated for the hot, humid regions of southeastern China (Chen et al. 2012a,b, Xu et al. 2013, Shi et al. 2015) because of the limited number of old-growth forests that exist in that area due to a long history of human activities. Indeed, it is quite challenging to find long tree-ring chronologies in this area.

Tree growth in subtropical (i.e. southeastern) China is often limited by low temperatures that occur during the winter and early spring prior to the start of the growing season (Shi et al. 2010, Chen et al. 2012a, Duan et al. 2012, 2013), whereas tree growth at sites with shallow soil is often limited by drought (Chen et al. 2012b, Dong et al. 2014). The complexity of growth patterns in response to climate highlights the need to study climate–growth relationships during different periods and in different regions of southeast China.

The climate of the southeastern coast of China is strongly influenced by atmospheric and oceanic circulations, such as the East Asia Summer Monsoon (EASM), El Niño-Southern Oscillation (ENSO), and Pacific Decadal Oscillation (PDO) (Chen et al. 2013a). The strength of EASM is one of the most important factors impacting China's summer precipitation (Ding et al. 2008), and the monsoon rainfall accounts for 40–50% of the annual precipitation in southeastern China (Zhou et al. 2009). Sea surface temperature (SST) anomalies that occur in the Pacific have a significant impact on the strength of the EASM (Ding et al. 2008, 2009, Chen et al. 2013a). ENSO also has a close relationship with the climate of China, such that the developing stage of a warm ENSO event results in drought in southern and northern China and flooding in central China; this relationship appears to be reversed in the decaying stage of a warm event (Huang & Wu 1989). Since the end of the 1970s, both the PDO and ENSO have moved from cold to warm phases (Li et al. 2013).

The climate fluctuations caused by atmospheric and oceanic circulation patterns can be well-captured by trees, especially those growing in coastal zones (Li et al. 2013, Xu et al. 2013). Previous studies of climate patterns based on tree-ring chronologies have found that ENSO has had different impacts on the climate of southeastern China during different periods (Xu et al. 2013); the same phenomenon has also been found in northwestern China (Yang et al. 2014). Fang et al. (2010) found that the reconstructed historical climate in north-central China was closely linked to the SSTs of the Indian Ocean and West Pacific. Li et al. (2013) reconstructed the variability of ENSO over the past 7 centuries based on 2222 tree-ring chronologies from the tropics and mid-latitudes of both hemispheres. D'Arrigo & Wilson (2006) reconstructed PDO history based on the tree-ring net in the high latitudes of Asia.

However, it is still unclear whether trees growing on the southeastern coast of China have recorded atmospheric–oceanic information, or how the shift in SSTs and abnormal atmospheric–ocean circulation has influenced the climate and tree growth in this region. In this study, we used tree-ring chronologies to investigate the time-varying climate–growth relationships of trees growing on the southeastern coast of China, and examined the influence of atmospheric and oceanic circulation on the climate and climate–growth relationships in this region. This study presents a tree-ring chronology of 210 yr of *Pinus massoniana* tree growth at Gu Mountain in Fuzhou City on the southeast coast of China for the first time, and is the nearest chronology to the coastal area of the East China Sea, and so is likely to have captured major atmospheric and oceanic circulation signals.

2. DATA AND METHODS

2.1. Study area climate and tree-ring sampling

Fujian Province is located on the southeast coast of China and has a typical subtropical marine monsoon climate. The Gu Mountain (GM) sample site (26.04°N, 119.24°E) is located in Fuzhou City, adjacent to the ocean (Fig. 1). Annual mean temperature and total precipitation in the area are 19.9°C and 1366 mm, based on data collected by the nearest meteorological station (Fuzhou Station) spanning 1953–2013. The climate of Fuzhou is characterized by the alternation of rainy and dry seasons. The rainy season extends from March to September and accounts for 81.2% of the annual precipitation (Fig. 2a). The highest amounts of precipitation fall during May and June. The typhoon season lasts from July to September and accounts for 31% of the annual precipitation, with high variability in rainfall. July is a relatively dry month, with comparatively little precipitation (137 mm) and the highest average monthly temperature (28.72°C). The second highest temperature occurs in August (28.48°C). July and August are also the months when extremely high temperature events frequently occur (Fig. 2b).

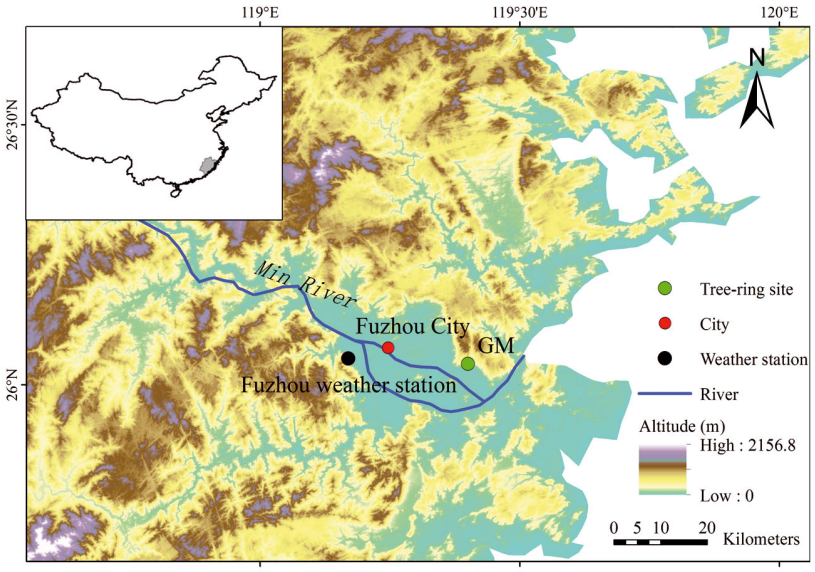

Fig. 1. Fujian Province in China, showing the location of the study region

GM is close to the centre of Fuzhou City and is a place of relaxation for local residents where trees are mainly found near the temple and are well protected. Old-growth *Pinus massoniana* is the dominant species in the forest; however, there are other species such as *Castanopsis carlesii* (Hemsl.) Hay and *Schima superba*. The youngest *P. massoniana* in the forest is more than 80 yr old with a diameter at breast height greater than ~40 cm. Shrubs and vines also grow in the forest and the soil is classified as Humic Acrisols with a high moisture content (Chen 2001).

A total of 186 tree-ring samples from 87 trees were collected from old-growth *P. massoniana*; 2 to 3 samples were collected from each tree using increment borers at different orientations. The samples were air-dried, finely sanded and cross-dated using standard dendrochronological techniques (Stokes & Smiley 1968). The exact calendar years of each growth ring were assigned through visual cross-dating (Fritts 1976). Tree rings were cross-dated, and the ring width measured to the nearest 0.001 mm using a linear table (LINTAB; RINNTECH) and the program TSAP-Win (Rinn 2003).

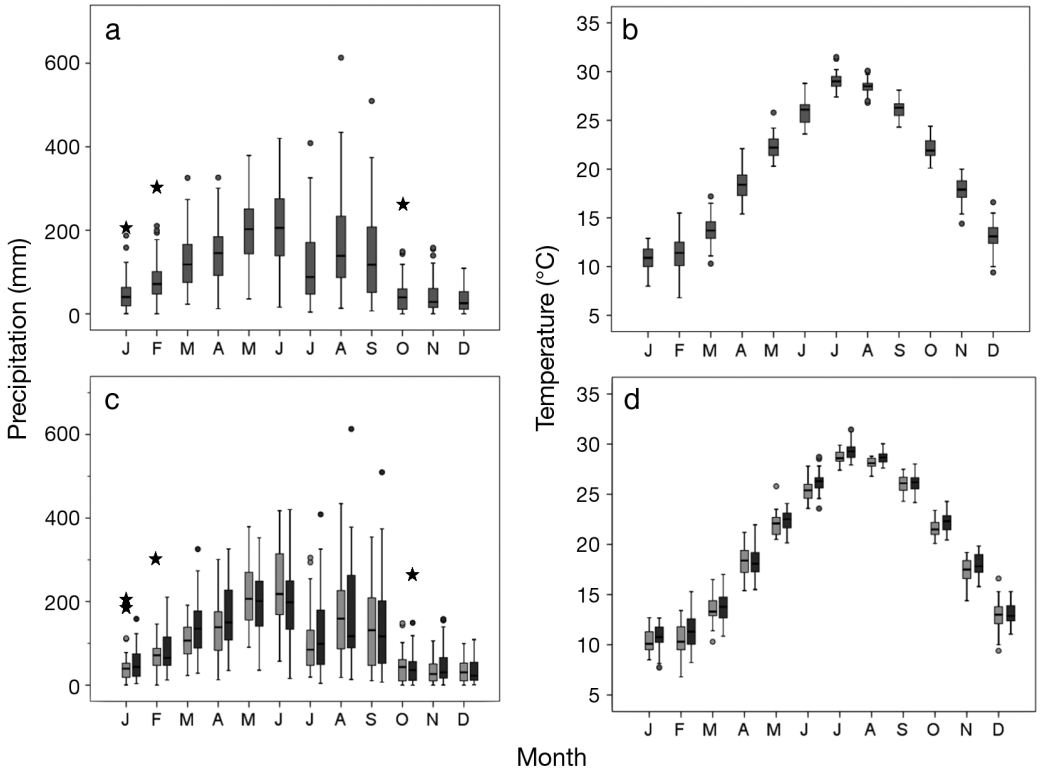

Fig. 2. Monthly total precipitation and mean temperatures in the research area based on Fuzhou weather station data from (a,b) 1953–2013, (c,d) 1953–1977 (light grey) and 1978–2013 (dark grey). Horizontal line in box: median (middle number of the data set, i.e. the monthly precipitation/temperature of the periods 1953–2013, 1953–1977 and 1978–2013). Top and bottom of box: 75th and 25th percentile of the data, respectively. Upper/lower whiskers: 75th/25th percentile ± 1.5 times the difference between the 75th and 25th percentile, indicating the main distribution range of the data set. Dots: extremes; asterisks: outliers

The program COFECHA (Homes 1983) was used to verify and control the cross-dating quality. Samples that exhibited abnormal growth, short ages and lower correlation with the main series were removed by combining the abnormal microhabitats of the trees inferred from photos and field records. A total of 119 tree-ring samples from 62 trees were retained for further analysis.

2.2. Tree-ring and climate data

The age-related growth trends were removed by using the ratio between the raw measurements and smoothing splines with a 50% frequency-response cutoff of two-thirds of the series length. The width measurements of ~12 trees showed growth releases in which the tree-ring width exhibited a sudden increase for ~20 yr and then gradually restored to a normal state. These growth releases were scattered among different segments in different trees and were more frequent in recent decades; they may have been caused by sudden increases in light and nutrients due to the natural death of adjacent trees, or by the creation of pathways in woods. The Friedman variable span smoother curve with a tweeter sensitivity of 5 was applied to remove these growth releases. Because each series was smoothed with a locally adaptive curve, it was useful in modeling the growth curves of the disturbed tree-ring series that did not evolve through time in a homogeneous way (Cook et al. 1995). Finally, the de-trended tree-ring series were averaged to generate a standard (STD) chronology through bi-weight robust-mean estimations (Cook 1985).

The chronology included the common and uncommon variance of the series. The expressed population signal (EPS) and subsample signal strength (SSS) were used to estimate the strength of the signal common to all trees, generally attributed to shared growth-limiting conditions, especially climate. EPS is defined by the mean inner-series correlation of all the series, while SSS is defined by the correlations between the mean of part of the series and the mean of all of the series (Wigley et al. 1984b). Thus, increasing EPS and SSS were tacitly associated with a more accurate estimation of climate–growth relationships, with values exceeding the suggested threshold of 0.85 leading to conclusions of a strong climate signal and an accurate climate sensitivity assessment (Mérian et al. 2013). The threshold of 0.85 in both SSS and EPS in this chronology corresponded to the reliable years of 1804 (14 samples) and 1805 (18 samples), respectively. Additionally, SSS was used to assess the robustness of the chronology, i.e. 1804 to 2013, 1 yr longer than EPS. The mean sensitivity (MS) of the chronology was 0.201, the first-order autocorrelation (AC1) was 0.675, and the all-series correlation was 0.280. The high values of the running means of EPS indicated that stable, common signals occurred for different segments (Wigley et al. 1984a) (Fig. 3). However, the running Rbar (a measure of the signal strength of the chronology) was relatively low (Fig. 3), which is a common phenomenon in subtropical climates (Chen et al. 2012b) and probably due to the relatively complacent growth of the trees.

Monthly precipitation and temperature (1953–2013) data were obtained from Fuzhou Station, which was the closest meteorological station. The EASM index (1948–2013) is an area-averaged seasonal (June–August, JJA) dynamical index at 850 hPa within the East Asian monsoon domain (10–40°N, 110–140°E) (Li & Zeng 2002). The PDO is a dominant internal oscillation in the climate system for Pacific areas, with phase shifts developing on decadal time scales. During the positive phase of the PDO, the upper oceans are warmer than during the preceding

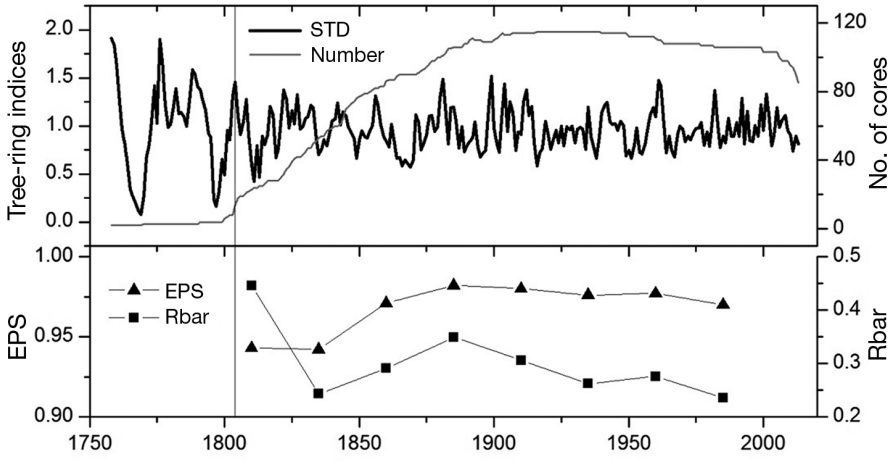

Fig. 3. The Gu Mountain chronology indices and the running Rbar (running based upon a 50 yr window with a 25 yr lag) and statistics of the running expressed population signal (EPS). The reliable portion of the chronology was determined by a subsample signal strength (SSS) value greater than 0.85 (vertical line: year [1804] when SSS is 0.5)

decades along the west coasts of North and South America and across the equatorial Pacific, and are colder over the western and central North Pacific (Graham 1994, Mochizuki et al. 2010). The ENSO index is represented by the Niño-3 SST, which is defined as the January–March SST anomaly averaged over the region (5°S–5°N, 90–150°W). The PDO index (December–February, DJF) for the period from 1901–2013, and ENSO indices (DJF) (Smith & Sardeshmukh 2000) for the period from 1872–2013 are available from www.cpc.ncep.noaa.gov/.

2.3. Data analysis

Relationships between the GM site tree-ring indices (STD) and climatic variables were analyzed by a correlation function, response function and partial correlation analysis. The response analyses can account for the multi-collinearity among monthly climatic parameters via a calculation of the relationships between tree rings and the major principal components (PCs) of the climate variables only. The response function analysis was performed using the program DendroClim2002 (Biondi & Waikul 2004), which employs a bootstrap procedure to evaluate significance level. Partial correlation analysis was performed by the 'Seascorr' method in MATLAB (MathWorks), which can separate the confounding influence of the intercorrelation of the primary and secondary climate variables (Meko et al. 2011). The climate–growth relationships were analyzed over the whole instrumental collection period (1953–2013) and in different climate backgrounds before and after the SST shift (i.e. the periods of 1953–1977 and 1978–2013). However, the 'Seascorr' analysis could not be performed on the 1953–1977 data because it was a period shorter than 30 yr (Meko et al. 2011). Climate–growth analyses were performed from the previous September to the current December in correlation and response function analyses, and from the previous November to the current December for the partial correlation analysis.

The correlation analysis among the GM chronology, PDO, ENSO and EASM was performed during their positive (1925–1946, 1978–2013) and negative (1890–1924, 1947–1977) PDO phases at interannual and interdecadal scales. The division of PDO positive/negative phases was inferred from previous studies based on the Pacific SST shift (Mantua et al. 1997, Minobe 1997).

A multi-taper method (MTM) spectral analysis was employed to examine the characteristics of drought variability in the frequency domain (Mann & Lees 1996). The significant spectra were determined based on a confidence level of 90% and the red noise assumption (Mann & Lees 1996).

3. RESULTS

For the period from 1953–2013, the correlation function analysis showed that the GM tree-ring indices were significantly and positively correlated with July ($p < 0.05$) and September precipitation ($p < 0.01$) (Fig. 4a), a result which was also evident in the response function analysis (Fig. 4b). The highest correlation with a seasonal climate variable occurred

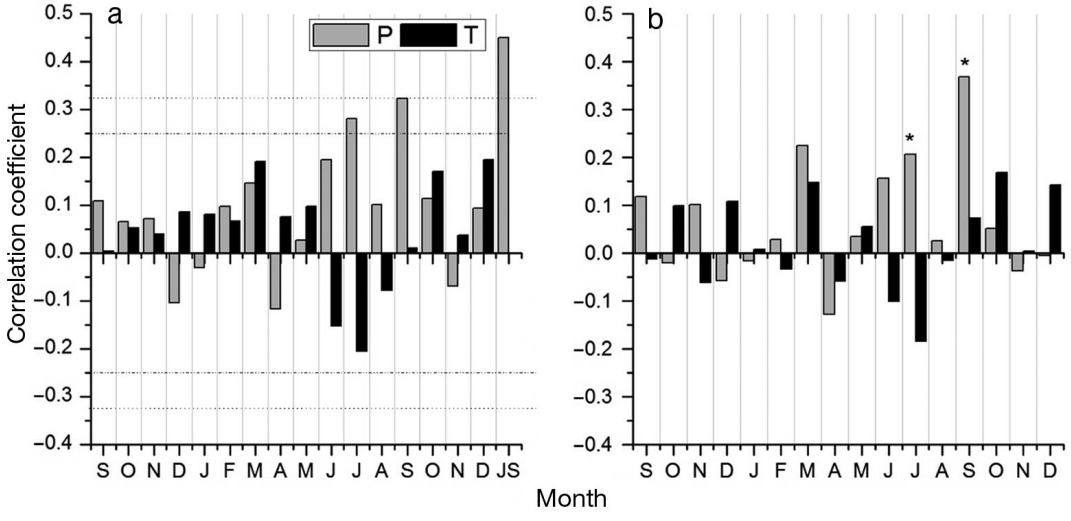

Fig. 4. Climate–growth (a) correlation function and (b) response function between Gu Mountain tree-ring chronology and precipitation (P) and temperature (T) from the Fuzhou weather station using data from September to December in the following year during the period from 1953–2013. JS: the combination of June to September (period with highest degree of statistical significance). Dashed and dotted lines: 95 and 99% confidence levels, respectively. *Values above 95% confidence level

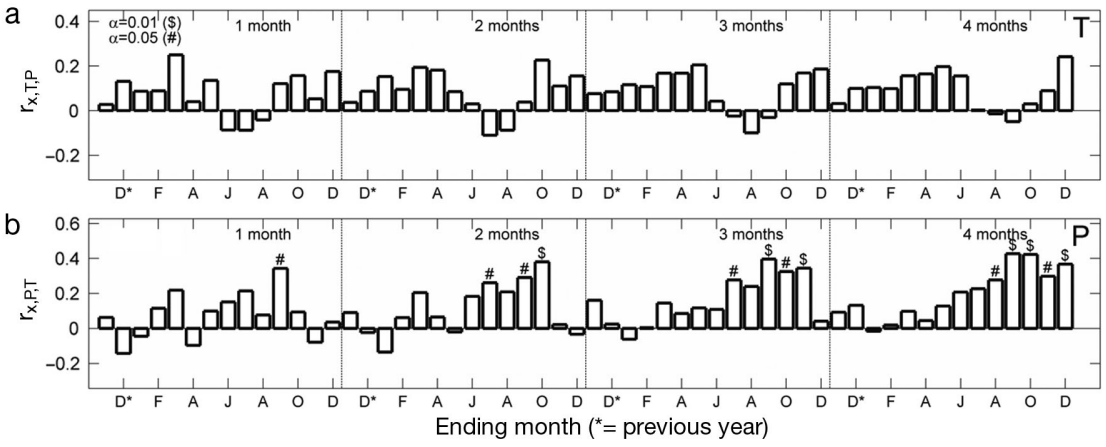

Fig. 5. Partial correlations between Gu Mountain chronology and (a) temperature with the influence of precipitation removed and (b) precipitation with the influenced of temperature removed, for the period of 1953–2013. $r_{x,T,P}$: partial temperature–growth correlation with precipitation unchanged; $r_{x,P,T}$: precipitation–growth correlation with temperature unchanged. 1, 2, 3, 4 months: seasonal climate variable averaged for 1, 2, 3, and 4 mo, respectively

with precipitation from June–September ($p < 0.01$) (Fig. 4a). Partial correlation analysis with precipitation alone (removing the influence of temperature) showed that there was still a significant positive correlation between September precipitation and tree-ring indices ($p < 0.05$) (Fig. 5b). The highest partial correlation with seasonal precipitation also occurred in June–September ($p < 0.01$) (Fig. 5b). Partial correlation analysis with temperature, removing the influence of precipitation, showed no significant relationship between temperature and tree-ring indices (Fig. 5a).

The tree-ring indices showed a significant positive correlation with previous and current September precipitation from 1953–1977, and the highest seasonal correlation appeared from June–September for precipitation ($p < 0.01$) (Fig. 6a). However, a significant positive correlation with tree-ring indices in June and September precipitation was found in the response function analysis (Fig. 6b).

For the 1978–2013 period, the tree-ring indices showed a significant positive correlation with January temperature and July precipitation, and a significant negative correlation with June and July temperature, although the highest seasonal correlation appeared from June–August for temperature ($r = -0.436$, $p < 0.01$) (Fig. 6c). In the response function analysis, a significant positive correlation only occurred for January temperature and July precipitation, and a significant negative correlation appeared for July temperature (Fig. 6d). The partial correlation between tree-ring indices and temperature, with the precipitation influence removed, showed a significant positive correlation with January and March temperatures ($p < 0.05$) and a significant negative correlation with July temperature ($p < 0.05$) (Fig. 7b). However, there was no significant correlation between tree-ring indices and precipitation in the partial correlation analysis when the influence of temperature was removed (Fig. 7a).

The MTM spectral analysis revealed that significant ($p < 0.01$) spectral peaks in the tree-ring chronology occurred at 2.6, 4.9, and 6.6 yr (Fig. 8). We also identified a cyclic pattern ($p < 0.1$) at 2.2, 2.5–2.7, 3.7, 4.1–5.0, 5.8–6.2, 6.5–7.3, 15.3–16.3, 17.4–19.7, and 21.8–33.0 yr (Fig. 8). The cycles of 2–8 yr may be related to ENSO (Allan et al. 1996), while the cycles of 17.4–19.7 and 21.8–33.0 years may have a relationship with the PDO (Mantua & Hare 2002).

The GM tree-ring chronology showed the same variances with the EASM, ENSO, and PDO indices in the common period and a significant positive correlation, especially on a decadal time scale (Table 1). A significant positive correlation of GM chronology with ENSO and PDO at the decadal time scale is shown in Fig. 9, except during the period of 1978–2013. However, a significant correlation was not found in the annual correlation analysis. A consistent positive correlation between GM and EASM was found both at an annual and decal timescale during the period of 1947–2013, and the coherency was enhanced in 1978–2013.

4. DISCUSSION

4.1. Climate–growth relationship

The similar patterns observed in the correlation (Fig. 4a) and response function analyses (Fig. 4b) for

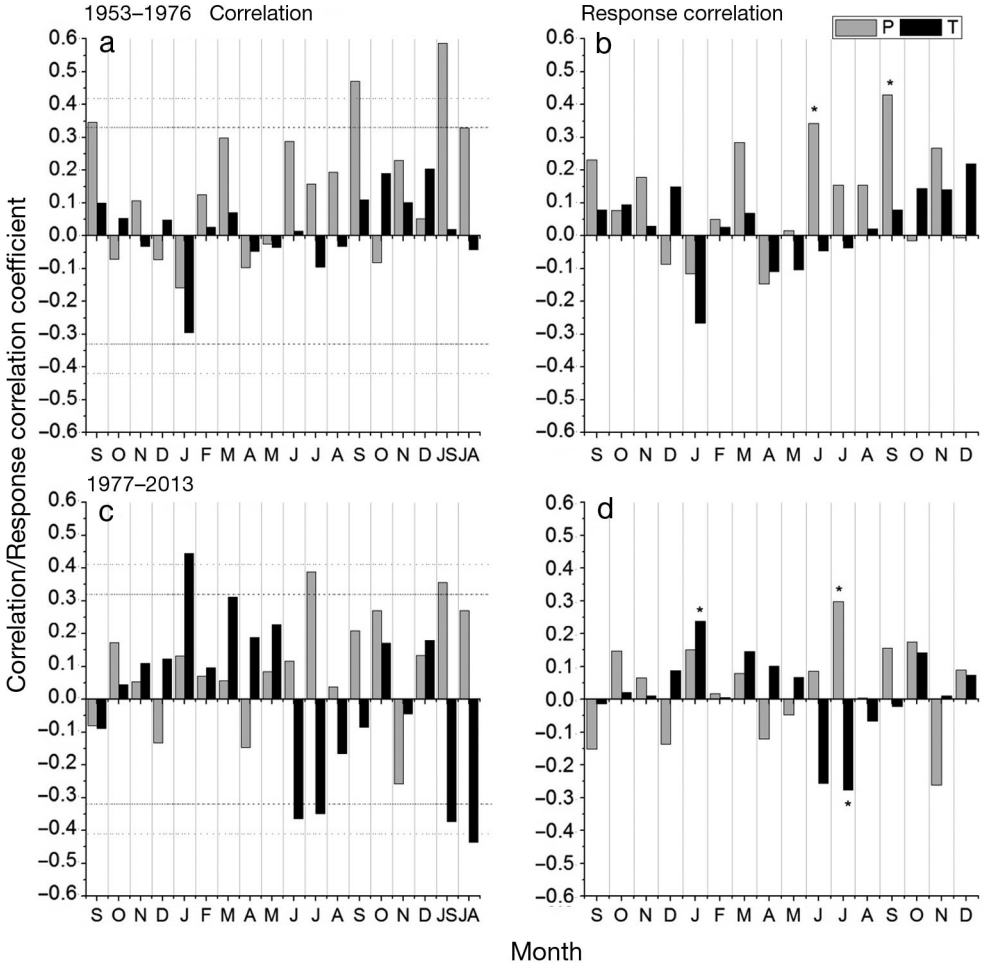

Fig. 6. (a,c) Climate–growth correlation function and (b,d) response function analysis between Gu Mountain tree-ring chronology and precipitation (P) and temperature (T) from the Fuzhou weather station showing data from September to December of the following year for the periods (a,b) 1953–1976 and (c,d) 1977–2013. JA and JS: the combination of data from June to August and June to September, respectively (periods with highest degree of statistical significance). Dashed and dotted lines: 95 and 99% confidence levels; respectively. *Values above 95% confidence level

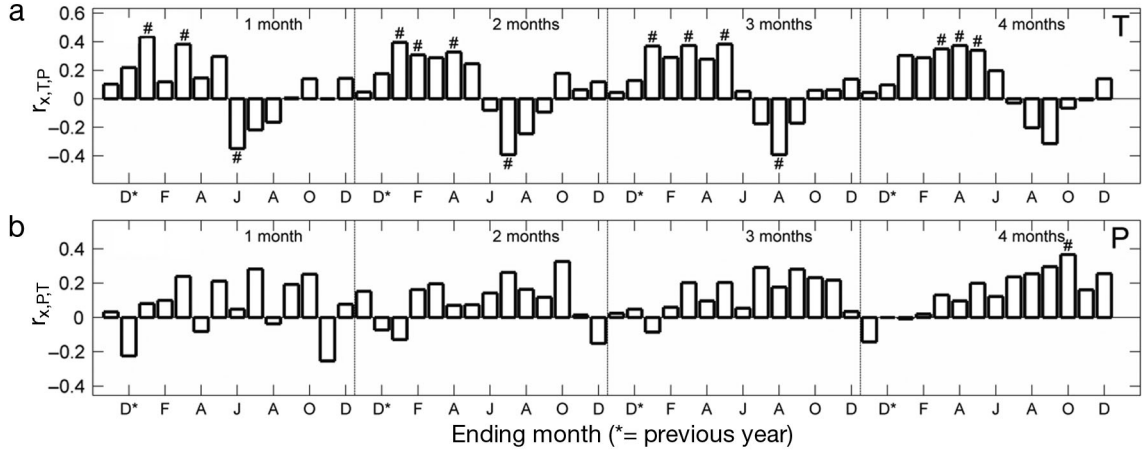

Fig. 7. Partial correlations between Gu Mountain chronology and (a) temperature with the influence of precipitation removed and (b) precipitation with the influence of temperature removed for the period 1978–2013; other details as in Fig. 5

the period from 1953–2013 indicate that July and September precipitation are the major limiting factors for tree growth (especially September) in southeastern coastal China. The significant positive correlation with September precipitation in the partial correlation analysis indicated the influence of September precipitation on growth beyond that explainable by the covariation of precipitation with temperature

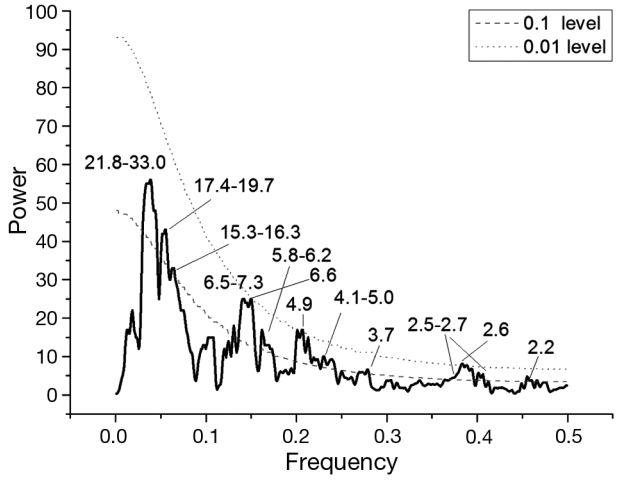

Fig. 8. Multi-taper spectral analysis of the tree-ring reconstruction and confidence limits at the 0.01 and 0.1 levels. Numbers/ranges: statistically significant cycles

(Fig. 5d). The high seasonal positive correlation with June–September precipitation indicated that summer drought severely limits tree growth, which is similar to the results of studies conducted in nearby Changting City (Chen et al. 2012b, Dong et al. 2014).

Table 1. Correlation coefficients of Gu Mountain (GM) tree-ring chronology with the El Niño-Southern Oscillation (ENSO), East Asia Summer Monsoon (EASM), and Pacific Decadal Oscillation (PDO) indices. *p < 0.05, **p < 0.01

	GM	GM (decadal time scale)	GM (annual time scale)
ENSO (n = 142)	0.113	0.354**	0.016
EASM (n = 66)	0.243*	0.321**	0.245*
PDO (n = 159)	0.167*	0.309**	0.048

July is the driest summer month with the highest temperature for this region (conditions that can result in summer drought); it is also an important month for tree growth. Thus, the lower amounts of precipitation can severely limit tree growth. Because late wood accounts for a large part of ring width (up to 2/3 of the total width) and mainly forms in September, a lack of precipitation in this month will limit late wood formation.

As shown in Fig. 6a,b, from 1953–1977 the tree-ring indices were generally positively correlated with precipitation, especially in June and September, but

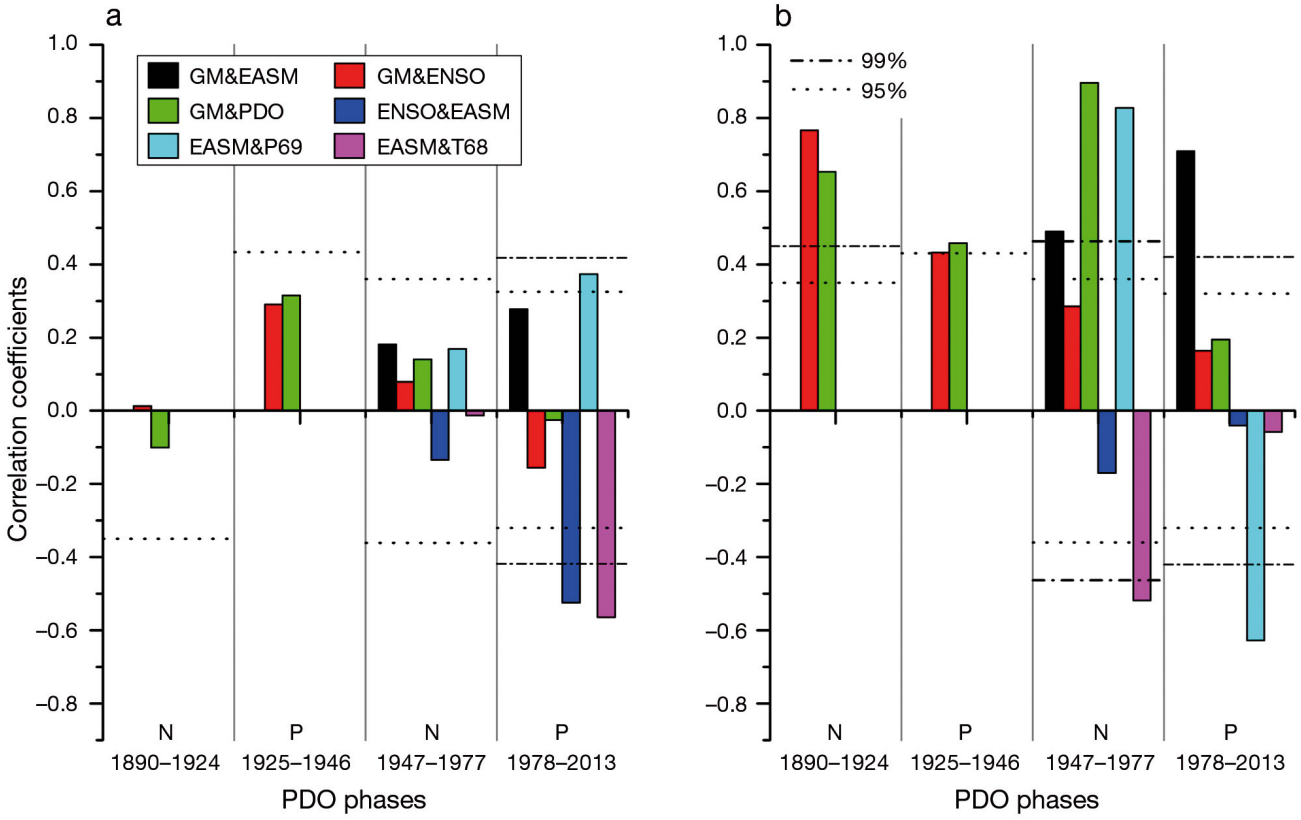

Fig. 9. The correlation of the Gu Mountain (GM) tree-ring chronology with EASM, ENSO and PDO indices, and the correlation of EASM with precipitation from June–September (P69) and temperature from June–August (T68) during the different PDO phases at (a) annual and (b) decal time scales

correlations with temperature are not so obvious. The greater the precipitation in June and September (the main growing season for trees in this area), the greater the promotion of tree growth as a premise of sufficient heat. Therefore, June and September precipitation were the main limiting factors for tree growth from 1953–1977.

A positive correlation with precipitation and a negative correlation with temperature during the summer months from 1978–2013 was more obvious than the corresponding correlations from 1953–1977 (Fig. 6c), suggesting an enhanced drought response in recent decades. This effect is also apparent in the increasing temperatures and heavy rainfall events and declining light rain for most months from 1978–2013, especially in July and August (Fig. 2c,d). A negative correlation with July temperatures and a positive correlation with precipitation indicate that drought in July severely limited tree growth with increasing temperature (Fig. 6c,d). Although the precipitation in July between 1978–2013 was slightly higher than the previous period, it tended to be composed mainly of heavy rainfall and storm rain, with few light rain events (Fig. 2c) (Cai et al. 2010). The loose, permeable soil in this area can only maintain a portion of the heavy precipitation, thus little of it is available for tree growth. Furthermore, the increasing temperature with more frequent extreme high temperature events could lead to strong evaporation (Fig. 2d). Therefore, the benefits of increasing precipitation during this period disappear, and the limits of drought on tree growth are more serious.

During June, the temperature clearly increases, with more extremely high temperature events (Fig. 2d), which would induce stomata to close and limit photosynthesis and tree growth (Figs. 6c,d & 7b). The June precipitation in 1978–2013 was less than that in 1953–1977, but it was still the highest monthly precipitation throughout the year with more light rain and more rain retention in the soil (Fig. 2c). Hence, June precipitation would provide less of a limitation for tree growth (Fig. 6c,d).

January is the coldest month of the year, and the positive correlation between January temperatures and tree-ring indices indicates that warmer temperatures could reduce the influence of cold snaps that occur in winter (Fig. 6c,d & 7b). A positive correlation was not shown in 1953–1977, even appearing as a negative (non-significant) correlation (Fig. 6a,b), although the mean temperature in 1953–1977 was colder than in 1978–2013 (Fig. 2d). However, the minimum temperature in January during 1978–2013 was lower than that in 1953–1977, with the occurrence of extreme low temperature events (Fig. 2d). Some studies have reported that cold surges are increasing because of the more fast-developing cases of Siberian Highs and the more frequent negative phase of the Arctic Oscillation during recent decades (Chen et al. 2004, Ou et al. 2015). Trees growing in a warm environment are more sensitive to cold events; thus, the more frequent cold events in January during 1978–2013 have severely limited tree growth (Duan et al. 2012, 2013). The significant positive correlation that was found with September precipitation disappeared in the latter period, which is probably because increased amounts of precipitation in the more recent period satisfied the requirements for tree growth (Fig. 2).

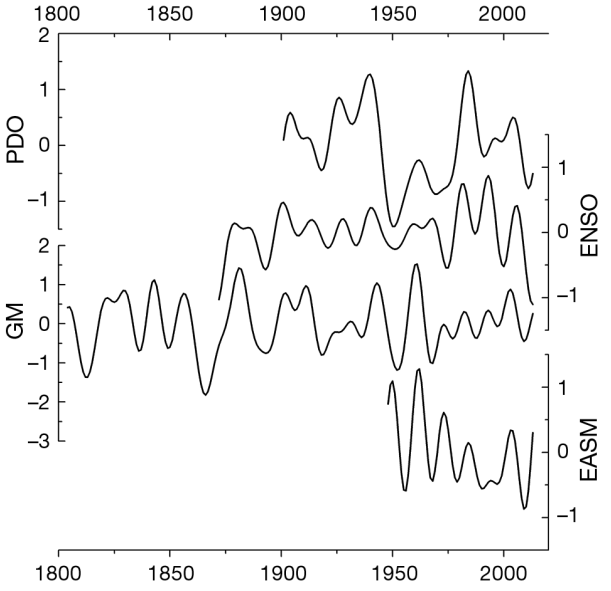

Fig. 10. Comparison of the Gu Mountain (GM) tree-ring chronology, EASM, ENSO and PDO indices using a 10 yr low frequency filter

4.2. Climate change and potential climate regimes

Consistent decadal (frequencies < 0.1) variations between GM tree-ring chronology and the EASM, ENSO and PDO indices indicate that the tree-ring variations are likely correlated with large-scale atmospheric–oceanic circulations (Fig. 10). We also found significant positive correlations of our tree-ring chronology with ENSO, PDO and EASM at the decadal time scale (Table 1). Additionally, the significant positive correlation between the GM chronology and EASM were significant both at annual and decadal time scales (Table 1).

ENSO is one of the most important modulators of the strength of EASM (Ding et al. 2008, 2009, Chen et al. 2013a), which can further impact precipitation and tree growth in our study area. At an annual time scale, ENSO was significantly negatively correlated with EASM from 1978–2013 ($p < 0.01$), but the correlation was not obvious during the 1947–1977 period (Fig. 9a). This indicates that a warm ENSO event can lead to a weak EASM, and that the influence is stronger in the positive PDO phases than in the negative PDO phases (Chan 2005). This same phenomenon was also found in a previous study, whereby the positive PDO phase would enhance the influence of warm ENSO events and usually lead to a dry monsoon (Chan 2005). EASM showed a significantly positive correlation with precipitation during June–September ($p < 0.05$) and a significant negative correlation with temperatures in June–August ($p < 0.01$) during 1978–2013, while a significant correlation was not found in 1947–1977 (Fig. 9a). This indicates that the influence of EASM on local precipitation and temperature is enhanced during the positive PDO phases when the influence of ENSO on EASM is enhanced.

At a decadal time scale, the GM chronology showed a significant positive correlation with EASM from 1947–2013. The correlation coefficient was higher in the positive PDO phase from 1978–2013 than in the negative phase from 1947–1977 despite a rising trend of the GM and a declining trend of EASM during this period. Previous studies have shown that with the weakening of EASM, the main rain center moves gradually southward with the increasing precipitation in southeast China (Ding et al. 2008, 2009), which is also evidenced by the significant negative correlation between EASM and precipitation in June–September from 1978–2013, and a significant positive correlation from 1947–2013 (Fig. 9b).

5. CONCLUSIONS

The GM tree-ring chronology spanning 1804–2013 from the southeastern coast of China is the closest tree-ring site to the ocean studied thus far in China, and so is likely to have captured major atmospheric and oceanic circulations signals. The lower amounts of precipitation and higher temperatures in summer limit tree growth in this area; precipitation during June–September was the main limiting factor for growth between 1953–1977. However, since 1978 the climate has been drier, with increasing temperature and decreasing light precipitation, and thus tree growth has been limited by high temperatures in the summer. At the same time, increasing cold snap events during the winter also limit tree growth; hence, tree-ring indices showed a significant positive correlation with January temperatures during the 1978–2013 period.

The GM chronology accurately reflected the fluctuations of ENSO, PDO, and EASM, especially on a decadal time scale. At an annual time scale, a warm ENSO causes a weak EASM in the positive PDO phase, and a weak EASM results in decreased amounts of precipitation and higher temperatures, which further limit tree growth. At the decadal time scale, weakening EASM has promoted tree growth by the center-southward movement of the monsoon rain since 1977.

Acknowledgements. This research was funded by the National Science Foundation of China (41471172, U1405231 and 41171039), non-profit research funds of Fujian Province (2014R1034-2) and the Fellowship for Distinguished Young Scholars of Fujian Province (2015J06008).

LITERATURE CITED

Allan R, Lindesay J, Parker D (1996) El Niño Southern Oscillation and climatic variability. CSIRO, Clayton

Biondi F, Waikul K (2004) DENDROCLIM2002: a C++ program for statistical calibration of climate signals in tree-ring chronologies. Comput Geosci 30:303–311

Cai Y, Qian W, Yang S, Lin Z (2010) Regional features of precipitation over Asia and summer extreme precipitation over Southeast Asia and their associations with atmosphere-oceanic conditions. Meteorol Atmos Phys 106: 57–73

Chan JCL (2005) PDO, ENSO and the early summer monsoon rainfall over south China. Geophys Res Lett 32: L08810, doi:10.1029/2004GL022015

Chen J (2001) Classification and distribution of mountainous soils in Fujian Province based on Chinese soil taxonomy. J Mountain Res 19:1–8 (in Chinese with English abstract)

Chen TC, Huang WR, Yoon J (2004) Interannual variation of the east Asian cold surge activity. J Clim 17:401–413

Chen F, Yuan YJ, Wei WS, Yu SL, Zhang TW (2012a) Tree ring-based winter temperature reconstruction for Changting, Fujian, subtropical region of Southeast China, since 1850: linkages to the Pacific Ocean. Theor Appl Climatol 109:141–151

Chen F, Yuan YJ, Wei WS, Yu SL, Zhang TW (2012b) Reconstructed temperature for Yong'an, Fujian, Southeast China: linkages to the Pacific Ocean climate variability. Global Planet Change 86-87:11–19

Chen W, Feng J, Wu R (2013a) Roles of ENSO and PDO in the link of the East Asian Winter Monsoon to the following Summer Monsoon. J Clim 26:622–635

Chen Z, Zhang X, He X, Davi NK, Cui M, Peng J (2013b) Extension of summer (June-August) temperature records for northern Inner Mongolia (1715-2008), China using

tree rings. Quat Int 283:21–29
Cook ER (1985) A time series analysis approach to tree ring standardization. PhD thesis, University of Arizona, Tucson, AZ
Cook E, Briffa K, Meko D, Graybill D, Funkhouser G (1995) The segment length curse in long tree-ring chronology development for paleoclimatic studies. Holocene 5: 229–237
D'Arrigo R, Wilson R (2006) On the Asian expression of the PDO. Int J Climatol 26:1607–1617
Ding Y, Wang Z, Sun Y (2008) Inter decadal variation of the summer precipitation in East China and its association with decreasing Asian summer monsoon. Part I: Observed evidences. Int J Climatol 28:1139–1161
Ding Y, Sun Y, Wang Z, Zhu Y, Song Y (2009) Inter-decadal variation of the summer precipitation in China and its association with decreasing Asian summer monsoon. Part II: Possible causes. Int J Climatol 29:1926–1944
Ding Y, Liu Y, Sun Y, Song Y (2010) Weakening of the Asian summer monsoon and its impact on the precipitation pattern in China. Int J Water Resour Dev 26:423–439
Dong Z, Zheng H, Fang K, Yan R, Zheng L, Yang Y (2014) Responses of tree-ring width of *Pinus massiniana* to climate change in Sanming, Fujian Province. J Subtropical Res Environ 9:1–7 (in Chinese with English abstract)
Duan J, Zhang QB, Lv L, Zhang C (2012) Regional-scale winter-spring temperature variability and chilling damage dynamics over the past two centuries in southeastern China. Clim Dyn 39:919–928
Duan J, Zhang QB, Lv LX (2013) Increased variability in cold-season temperature since the 1930s in subtropical China. J Clim 26:4749–4757
Fang K, Gou X, Chen F, D'Arrigo R, Li J (2010) Tree-ring based drought reconstruction for the Guiqing Mountain (China): linkages to the Indian and Pacific Oceans. Int J Climatol 30:1137–1145
Fritts HC (1976) Tree rings and climate. Academic Press, New York, NY
Gou X, Chen F, Cook E, Jacoby G, Yang M, Li J (2007) Streamflow variations of the Yellow River over the past 593 years in western China reconstructed from tree rings. Water Resour Res 43:W06434, doi:10.1029/2006WR005705
Graham N (1994) Decadal-scale climate variability in the tropical and North Pacific during the 1970s and 1980s: observations and model results. Clim Dyn 10:135–162
Homes RL (1983) Computer-assisted quality control in tree-ring dating and measurement. Tree-Ring Bull 43:51–67
Huang R, Wu Y (1989) The influence of ENSO on the summer climate change in China and its mechanism. Adv Atmos Sci 6:21–32
Hughes MK, Swetnam TW, Diaz HF (eds) (2011) Dendroclimatology: progress and prospects. Developments in paleoenvironmental research, Vol 11. Springer, New York, NY
Li JP, Zeng QC (2002) A unified monsoon index. Geophys Res Lett 29:1274, doi:10.1029/2001GL013874
Li J, Xie SP, Cook ER, Morales MS and others (2013) El Niño modulations over the past seven centuries. Nat Clim Change 3:822–826
Liang E, Shao X, Eckstein D, Liu X (2010) Spatial variability of tree growth along a latitudinal transect in the Qilian Mountains, northeastern Tibetan Plateau. Can J For Res 40:200–211
Liu Y, Tian H, Song H, Liang J (2010) Tree ring precipitation reconstruction in the Chifeng-Weichang region, China, and East Asian summer monsoon variation since A.D. 1777. J Geophys Res 115:D06103, doi:10.1029/2009JD012330
Liu H, Park Williams A, Allen CD, Guo D and others (2013) Rapid warming accelerates tree growth decline in semi-arid forests of inner Asia. Glob Change Biol 19: 2500–2510
Liu XH, Xu GB, Griessinger J, An WL and others (2014) A shift in cloud cover over the southeastern Tibetan Plateau since 1600: evidence from regional tree-ring ^{18}O and its linkages to tropical oceans. Quat Sci Rev 88:55–68
Mann ME, Lees JM (1996) Robust estimation of background noise and signal detection in climatic time series. Clim Change 33:409–445
Mantua NJ, Hare SR (2002) The Pacific Decadal Oscillation. J Oceanogr 58:35–44
Mantua NJ, Hare SR, Zhang Y, Wallace JM, Francis RC (1997) A Pacific interdecadal climate oscillation with impacts on salmon production. Bull Am Meteorol Soc 78: 1069–1079
Meko DM, Touchan R, Anchukaitis KJ (2011) Seascorr: a MATLAB program for identifying the seasonal climate signal in an annual tree-ring time series. Comput Geosci 37:1234–1241
Mérian P, Pierrat JC, Lebourgeois F (2013) Effect of sampling effort on the regional chronology statistics and climate–growth relationships estimation. Dendrochronologia 31:58–67
Minobe S (1997) A 50-70 year climatic oscillation over the North Pacific and North America. Geophys Res Lett 24: 683–686
Mochizuki T, Ishii M, Kimoto M, Chikamoto Y and others (2010) Pacific decadal oscillation hindcasts relevant to near-term climate prediction. Proc Natl Acad Sci USA 107:1833–1837
Ou T, Chen D, Jeong JH, Linderholm HW, Zhou T (2015) Changes in winter cold surges over southeast China: 1961 to 2012. Asia-Pac J Atmospheric Sci 51:29–37
Rinn F (2003) TSAP-Win: software for tree-ring measurement, analysis and presentation. RINNTECH, Heidelberg. www.rinntech.com
Shao X, Xu Y, Yin ZY, Liang E, Zhu H, Wang S (2010) Climatic implications of a 3585-year tree-ring width chronology from the northeastern Qinghai-Tibetan Plateau. Quat Sci Rev 29:2111–2122
Shi J, Cook ER, Lu H, Li J, Wright WE, Li S (2010) Tree-ring based winter temperature reconstruction for the lower reaches of the Yangtze River in southeast China. Clim Res 41:169–176
Shi J, Lu H, Li J, Shi S, Wu S, Hou X, Li L (2015) Tree-ring based February-April precipitation reconstruction for the lower reaches of the Yangtze River, southeastern China. Global Planet Change 131:82–88
Smith CA, Sardeshmukh PD (2000) The effect of ENSO on the intraseasonal variance of surface temperatures in winter. Int J Climatol 20:1543–1557
Stokes MA, Smiley TL (1968) An introduction to tree-ring dating. University of Chicago Press, Chicago, IL
Wigley TML, Briffa KR, Jones PD (1984a) Average value of correlated time series, with applications in dendroclimatology and hydrometeorology. J Appl Meteorol Climatol 23:201–234
Wigley TML, Briffa KR, Jones PD (1984b) On the average value of correlated time series, with applications in

dendroclimatology and hydrometeorology. J Clim Appl Meteorol 23:201–213

Xu C, Zheng H, Nakatsuka T, Sano M (2013) Oxygen isotope signatures preserved in tree ring cellulose as a proxy for April-September precipitation in Fujian, the subtropical region of southeast China. J Geophys Res 118:12805–12815

Yang B, Kang S, Ljungqvist FC, He M, Zhao Y, Qin C (2014) Drought variability at the northern fringe of the Asian summer monsoon region over the past millennia. Clim Dyn 43:845–859

Zhang QB, Evans MN, Lyu L (2015) Moisture dipole over the Tibetan Plateau during the past five and a half centuries. Nat Commun 6:8062, doi:10.1038/ncomms9062

Zhou T, Gong D, Li J, Li B (2009) Detecting and understanding the multi-decadal variability of the East Asian Summer Monsoon: recent progress and state of affairs. Meteorologische Zeitschrift 18:455–467

Editorial responsibility: Gouyu Ren, Beijing, China

Submitted: July 13, 2015; Accepted: January 12, 2016
Proofs received from author(s): February 22, 2016